Bull. Mater. Sci. (2021)44:245
https://doi.org/10.1007/s12034-021-02537-9

Potential biomedical application of a new MOF based on a derived PET: synthesis and characterization

DENIS A CABRERA-MUNGUIA[1,*], M ILEANA LEÓN-CAMPOS[1], JESÚS A CLAUDIO-RIZO[1], DORA A SOLÍS-CASADOS[2], TIRSO E FLORES-GUIA[1] and LUCIA F CANO SALAZAR[1]

[1]Materiales Avanzados, Facultad de Ciencias Químicas, Universidad Autónoma de Coahuila, Ing. J. Cárdenas s/n, 25280 Saltillo, Coah, México

[2]Centro Conjunto de Investigación en Química Sustentable, UAEM-UNAM, carr. km 14.5 unidad San Cayetano Toluca-Atlacomulco, 50200 Toluca, Edo. Mex., México

*Author for correspondence (dcabrera@uadec.edu.mx)

MS received 2 November 2020; accepted 15 June 2021

Abstract. Metal–organic frameworks (MOFs) are materials with a large surface area and antimicrobial properties are advantageous properties for the controlled release of molecules for biomedical applications. However, their synthesis is expensive and harmful to the environment due to the use of organic ligands and solvents. Thus, this work proposes the synthesis of a new MOF by hydrothermal method using water as the solvent, aluminium nitrate as a metallic source, and bis(2-hydroxyethyl) terephthalate (BHET) as organic ligand, obtained via glycolysis of polyethylene terephthalate (PET); and its comparison with MIL53-Al MOF, synthesized from terephthalic acid (BDC) as organic ligand. Both MOFs were characterized by XRD, ATR-FTIR, N_2 physisorption, TGA, SEM and XPS; besides their *in vitro* biocompatibility was tested by porcine fibroblasts viability. The results indicate that aluminium ions are coordinated to both carbonyl and hydroxyl functional groups of the BDC and BHET organic ligands. The new BHET-Al MOF shows higher thermal stability than MIL53-Al, it also exhibits a macroporous structure in comparison with the microporosity of the MIL53-Al. BHET-Al MOF is not cytotoxic for porcine dermal fibroblasts growing on its surface for up to 48 h of culture, thus, this innovative MOF is a promising material for the controlled release of drugs.

Keywords. BHET; MOFs; MIL-53; aluminium; cytotoxicity.

1. Introduction

The metal–organic frameworks (MOFs) are coordination polymers constituted by a metallic centre (e.g., Zn^{+2}, Al^{+3}, Fe^{+3} and Zr^{+4}) and an organic ligand (e.g., terephthalic acid, trimesic acid and 2-methylimidazole). These materials are characterized to present high thermal stability and large surface area, because of this, they have been widely applied as adsorbent (e.g., drugs, CO_2, colourants and heavy metal ions), catalysts (bifunctional materials with the simultaneous presence of both Lewis acid and base), and recently as biocompatible materials with antimicrobial properties [1].

Typically, MOFs are synthesized by hydrothermal method, where the inorganic structures $MO_n(OH)_m$ are coordinately bonded to an organic ligand with functional groups acting as Lewis base present in its chemical structure, such as $–NH_2$, –OH, –C=O and $–COO^-$. However, the organic ligands are usually very expensive, and they have cytotoxic character [2].

On the other hand, polyethylene terephthalate (PET) is a solid residue produced and consumed in huge amounts by human activity. PET is classified as a thermoplastic due to its resistance to degradation or hydrolytic cleavage of chemical bonds, thus, the PET is considered a non-biodegradable plastic [3]. To overcome this problem, PET can be depolymerized via glycolysis with ethylene glycol to obtain bis(2-hydroxyethyl) terephthalate ($HO–C_2H_4–OOC–C_6H_4–COO–C_2H_4–OH$, BHET) as the esterification product under the presence of a Lewis catalyst [4]. The development of synthesis strategies for novel materials based on BHET, represents a sustainable alternative. The BHET compound possesses a very similar chemical structure to terephthalic acid ($HOOC–C_6H_4–COOH$, BDC), widely used as a ligand for the generation of the representative MIL53-Al MOF, however, the presence of end hydroxyl groups in BHET allows its easier dissolution in water than the non-polar BDC, an advantage that can be used to avoid the use of toxic solvents in the synthesis of MOFs, thus, improving its potential application in biomedical strategies.

The present work describes an innovative and sustainable strategy to generate novel MOFs with improved structure and properties for biomedical applications, taking advantage of the high solubility of BHET in the aqueous medium, thus, avoiding the use of toxic organic solvents. In the

Published online: 06 September 2021

present study, it is proposed the synthesis of a new MOF based on aluminium nitrate and BHET as organic ligand, which was obtained from PET depolymerization. Its structure, physicochemical properties and cytotoxicity were compared with its analogous MIL53-Al MOF, synthesized under the same reaction conditions.

2. Experimental

2.1 *Synthesis of BHET and MOFs*

The BHET compound was synthesized by depolymerization of PET, collected from waste bottles. In the general procedure, 10 g of powdered PET was placed into a ball flask with 50 ml of ethylene glycol and 0.2 wt% of Zn^{+2} (0.2 g). Then, the ball flask was collocated in a reflux system at 110°C for 8 h. The yielded product was precipitated with cold water, recovered by vacuum filtration and dried in an oven at 40°C [4].

The MIL53-Al MOF was typically synthesized by mixing 35 mmol of aluminium nitrate nonahydrate ($Al(NO_3)_3{\cdot}9H_2O$) and 17.5 mmol of BDC in 50 ml of distilled water [5]. The obtained solution was placed in a Teflon-lined steel autoclave and heated at 200°C for 72 h. The hydrothermal reactor was cooled down at room temperature, the white precipitate was filtrated under vacuum and was washed with distilled water to remove the nitric acid formed. The precipitate was dried at 80°C for 24 h (figure 1a).

The BHET-Al MOF was synthesized similarly to the procedure mentioned above replacing BDC with BHET, obtaining a yellowish solid (figure 1b).

2.2 *Characterization*

XRD patterns of BHET, BDC, BHET-Al and MIL-53 materials were acquired in a SAXS-Emc2, Anton Paar diffractometer in a 2θ range from 5 to 40° with a CuKα X-ray source (λ = 1.540 Å). Infrared spectroscopic spectra of BHET, BDC, BHET-Al and MIL53-Al materials were obtained by attenuated total reflection (FTIR–ATR) in Frontier equipment with a Perkin Elmer system, the spectra were acquired with a resolution of 16 cm^{-1} in the interval of 4000–650 cm^{-1}. The surface area of BHET-Al and MIL53-Al were determined by N_2 adsorption using BET method, performing the nitrogen physisorption experiments in a Quantachrome Autosorb iQ instrument with previous outgassing of the samples at 200°C during 12 h. For the thermogravimetric analysis (TGA), a TGA-4000 Perkin Elmer thermal analyzer was used, where 5 mg of sample was heated from room temperature to 800°C with a heating rate of 20°C min^{-1}, and an N_2 flow of 20 ml min^{-1} as inert atmosphere. The SEM micrographs were acquired in a JEOL JSM-6510LV SEM.

The X-ray photoelectron analysis (XPS) was carried out using a JEOL photoelectron spectrometer model JPS-9200 equipped with a monochromatic Mg X-ray radiation (300 W, 15 kV and 1253.4 eV). The BHET-Al and MIL53-Al powders were deposited on a conducting scotch tape and studied without any pre-treatment. The samples were in Al tapes on stainless-steel sample holders, which remained in a pre-analysis chamber until a pressure of 10^{-3} mbar was achieved before entering the analysis chamber. Survey spectra were recorded from 0 to 1100 eV at constant pass energy of 100 eV, onto 900 μm^2 of analysis area; narrow spectra of C1s, O1s and Al2p regions were recorded in the constant pass energy mode at 20 eV, dwell 100 and 10 scans at least. Charge correction was adjusted with carbon signal C1s 284 eV. Specsurf version 1.8.2 was used for acquisition and Origin v.8.2 for data analysis. A Shirley-type background was subtracted as the baseline from the spectra and the signal was deconvoluted using Gaussian curves to determine binding energies of different element core levels. NIST database was used to identify the corresponding element of the measured binding energies.

2.3 *Cytotoxicity test*

Dermal porcine fibroblasts (derived from a primary culture) were cultivated in culture plated and incubated in a humidified atmosphere with 95 and 5% of CO_2 at 37°C using as culture medium DMEM supplemented with foetal bovine serum (10% v/v) (CAISSON Labs). To every well containing the MOF (3 mg) in 3 ml of phosphate buffer (PBS 1X), the control (PBS 1X) was added a cellular suspension of 50,000 cells. The culture plates were incubated for 24 and 48 h. Then, the cellular viability of fibroblasts was determined by the capacity of these cells with active metabolism to reduce (3-(4,5-dimethylthiazol-2-yl)-2,5-diphenyltetrazolium bromide) MTT salt into insoluble formazan. The MTT solution (1 wt%) was also added to every well that contains MOFs suspension and control, the culture plates were maintained at 37°C for another 3 h to allow the reduction of MTT. The purple-coloured solutions (by formazan crystals generated) were dissolved in 2 ml of 2-propanol and characterized by UV–Vis measuring the absorbance of every solution at 560 nm, using a Synergy HTX Multi-Mode Reader, Biotek instrument. In this case, the absorbance of the purple-coloured solutions that come from the cell cultivated in the control represents 100% of fibroblast viability.

All cytotoxicity experiments were independently carried out at least three times. Mean and standard deviation are presented for each data set. Data sets were compared using ANOVA. The difference of the means was checked with a Tukey test and was considered statistically significant at a level of $P < 0.05$.

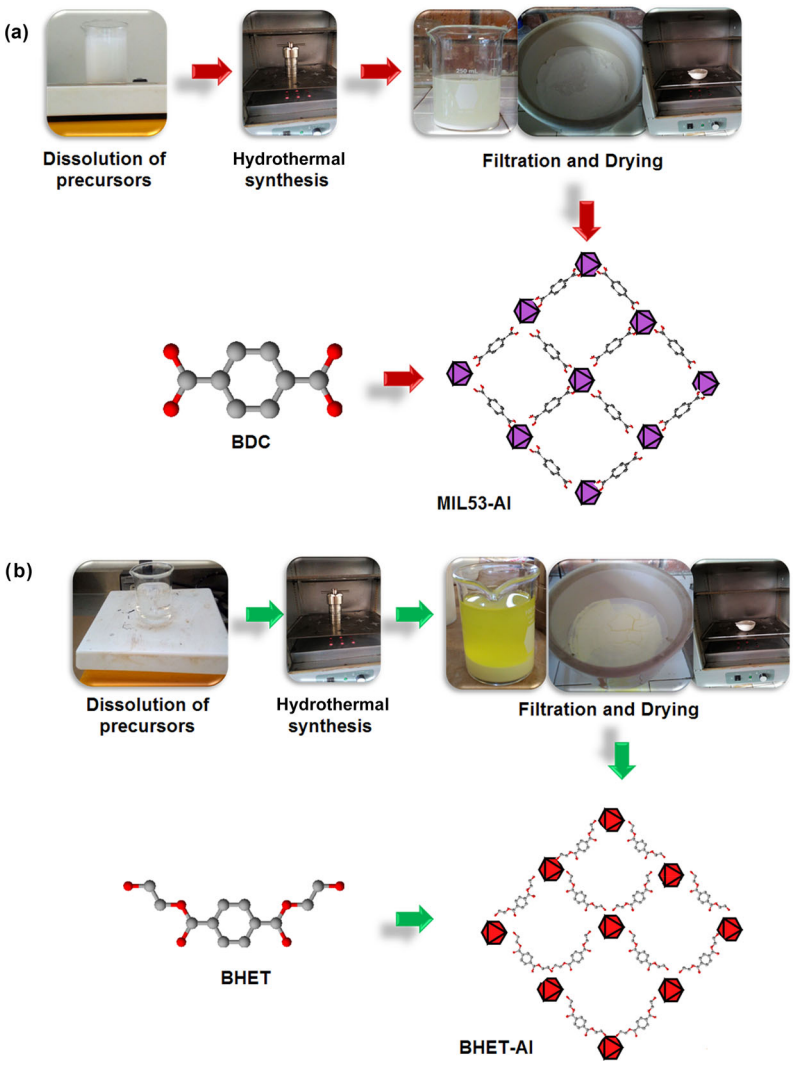

Figure 1. Synthesis procedure of (**a**) MIL53-Al and (**b**) BHET-Al MOFs.

3. Results and discussion

The X-ray diffractograms of the MOFs precursors are shown in figure 2a. The XRD of BDC indicates intense and well-defined signal peaks at 2θ = 17.3, 25.1 and 27.8° which belong to the crystallographic planes $(1\bar{1}0)$, (001) and $(11\bar{1})$ which is representative of a crystal packing of the infinite double hydrogen-bonded molecular chains obtaining materials in the form of plates and needles [6]. The XRD of BHET shows characteristics peaks at 2θ = 10.2, 16.3, 21.1, 23.3 and 27.4° that demonstrated a crystalline structure [7]. The diffraction signals found for BHET correlate with those for BDC, indicating that this PET derivative can also crystallize into needle-like structures. However, the presence of ethoxylated regions in BHET tends to generate structures with a lower crystalline order, considerably reducing the intensity of the diffraction signals, as can be seen in figure 2a.

The X-ray diffractograms of MIL53-Al and BHET-Al MOFs (figure 2b) exhibit the presence of the crystallographic planes at (2 0 0), (0 1 1), (3 0 2) and (0 2 0) that correspond to the signal peaks at 2θ = 10.2, 15.1, 21.2 and 26.9° that are related to crystalline structures with rhombohedral geometry. These diffraction peaks are involved in the coordination bonds formed among the aluminium ion with both hydroxyl (OH–) and carbonyl (C=O) functional groups of the ligands [8]. The only additional peak of the BHET-Al MOF is at 2θ = 38.2° indicating the formation of new crystalline planes related to coordination bonds among the aluminium ion with the ethoxy groups present in the BHET structure. In addition, the XRD of BHET-Al compared with MIL53-Al shows a semicrystalline material with

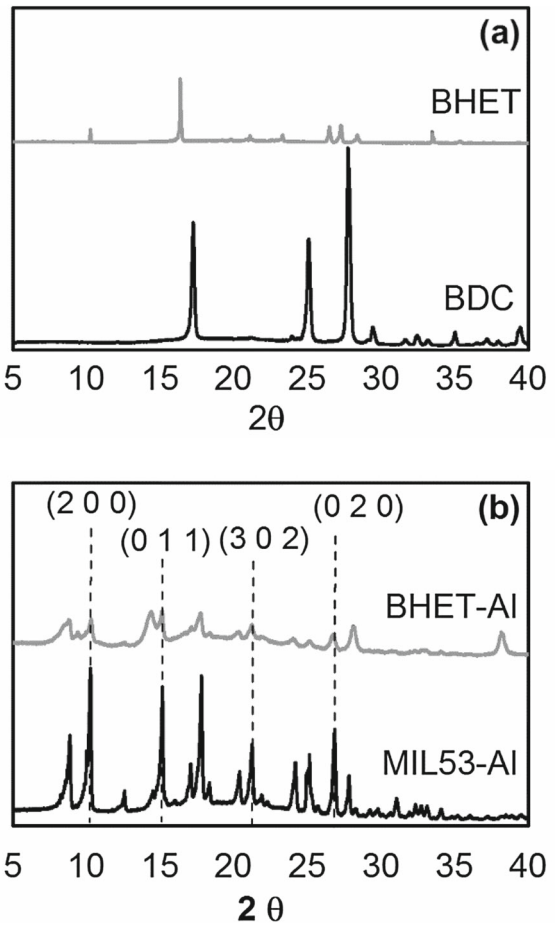

Figure 2. XRD of (**a**) BDC and BHET organic ligands and (**b**) MIL53-Al and BHET-Al MOFs.

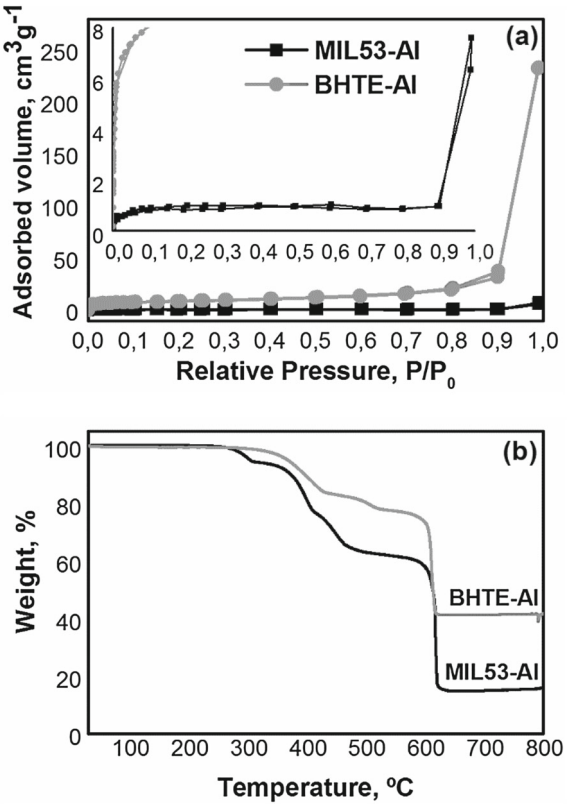

Figure 3. (**a**) N_2 physisorption isotherms and (**b**) thermogravimetric analysis of MIL53-Al and BHET-Al MOFs.

a smaller crystal size than MIL53-Al. It can also be seen in figure 2b that the reduction in the intensity and the distortion of the shape of the diffraction peaks for the BHET-Al, indicate that this MOF is packed in a lower crystalline order than MIL53-Al, which is associated with the presence of hydrophobic zones characterized by ethyl substituents present in the BHET structure, thus, generating structures with less crystallinity.

The N_2 physisorption isotherms of MIL53-Al and BHET-Al (figure 3a) show in both cases a type IV isotherm with a hysteresis loop type II, which is typical of non-porous solids, macropore adsorbents, and in some cases microporous materials [9]. The analysis of the surface area and pore size distribution exhibits a surface area of 1148 $m^2\ g^{-1}$, a micropore diameter in a range of 0.7–1.2 nm, and a mesopore diameter of 4.5 nm, which is in line with the values reported in the literature of $\sim$1100 $m^2\ g^{-1}$ and a pore diameter of 0.85 nm, for the representative MIL53-Al MOF [8,10]. Contrary to this, the BHET-Al MOF presents a surface area of 114 $m^2\ g^{-1}$ which is 10 times lower than MIL53-Al material, this area reduction is explained by a macropore distribution with a random size pore of 100 nm (0.1 μm). The hydrophobic regions represented by the ethyl substituents in the BHET structure propitiate those molecular aggregates interact with longer separation distances, generating macroporous structures with a lower surface area. This distortion in pore size can be used for encapsulation of molecules with biomedical interest, and to favour the diffusion of nutrients and oxygen in *in vitro* cellular systems.

TGA of both MOFs is represented in figure 3b; the thermograms show typical mass loss curves for MIL53-Al material [8,11]. The thermogram for MIL53-Al presents at 300°C a mass loss of 5.5% that is attributed to the loss of residual BDC present in MIL53-Al MOF. In addition, in the temperature range of 300–520°C, it is observed in both materials that the endothermic decomposition of organic matter with a mass loss of 38 and 22% for MIL53-Al and BHET-Al, respectively. At 600°C, it is observed that the formation of inorganic ashes with a mass loss of 86 and 58% for MIL53-Al and BHET-Al, respectively. Then, BHET-Al possesses higher thermal stability than MIL53-Al, this result indicates that there are higher coordination interactions among BHET precursor and aluminium ions than with BDC ligand. Both alkoxy and carbonyl functional groups behave as better Lewis bases in the BHET structure, generating coordination interactions more stable, requiring higher temperature to break these interactions for promoting the endothermic degradation of organic matter. It is also important to note that the resulting inorganic ashes are in an

order of 28% higher in BHET-Al than MIL53-Al, evidencing a higher presence of aluminium ions interacting with this derivative of PET, than with the precursor ligand of MIL53-Al. The high solubility of BHET precursor in water provides its high capacity for interaction with Al^{+3} ions, generating MOFs with improved thermal degradation.

The micrographs from SEM of MIL53-Al and BHET-Al materials (figure 4) exhibit rhomboid-shaped crystals for both materials with average size particles between 5–10 µm as is reported in the literature [12,13]. However, in the case of BHET-Al material, the rhombohedral crystals have a lower size than MIL53-Al crystals with embedded ultrathin lamellar structures that resemble boehmite morphology (AlOOH) [14]. In addition, BHET-Al rhomboid-shaped crystals generate agglomerates related to the presence of hydrogen bond effects between the ethoxylated ends of BHET.

The ATR–FTIR spectra of BDC and BHET precursors (figure 5a) due to their similar chemical structure share the same bands at $\sim$1720 cm^{-1} which belong to the carbonyl

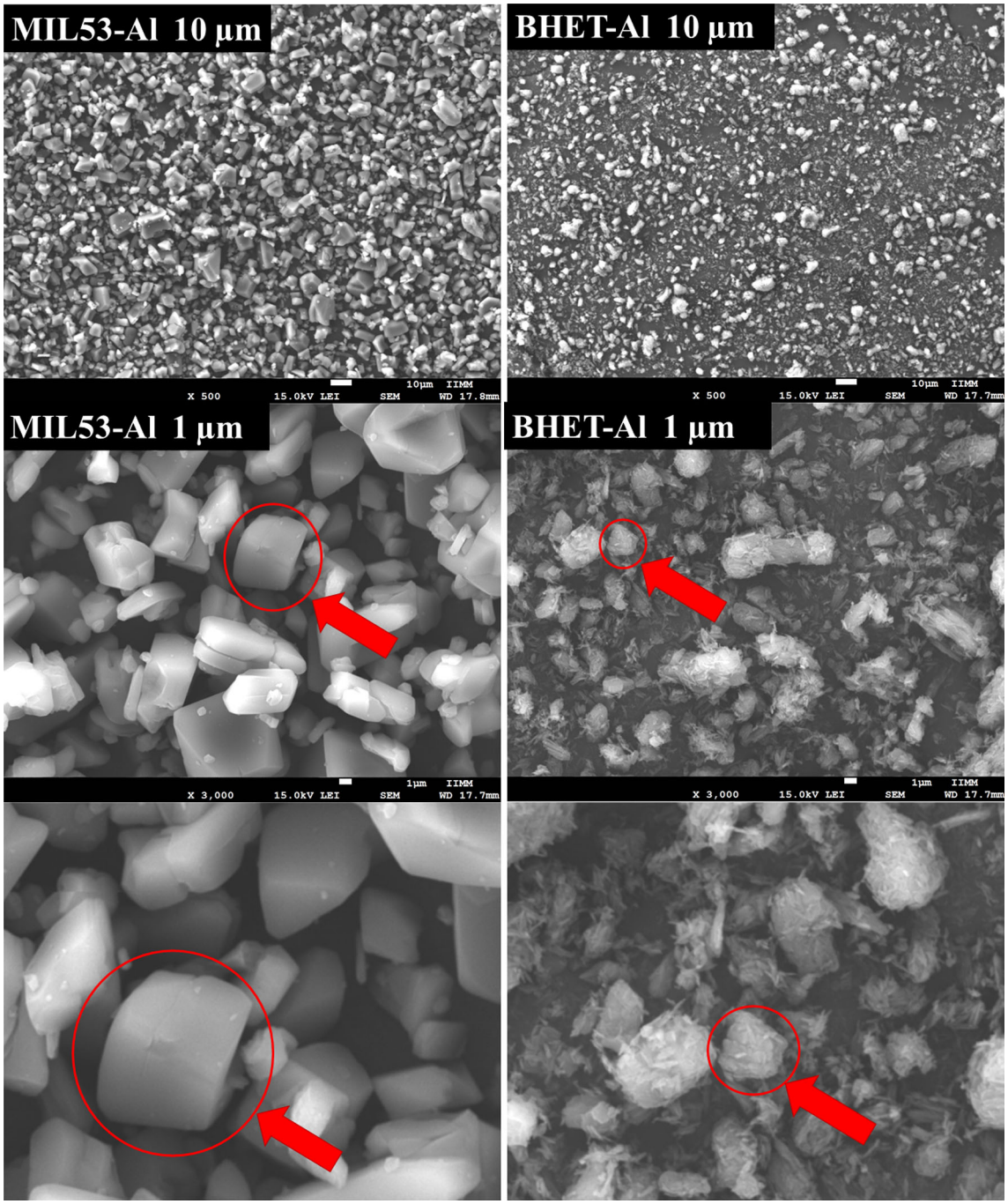

Figure 4. SEM micrographs of MIL53-Al (left) and BHET-Al (right) at 10 and 1 µm (from top to bottom).

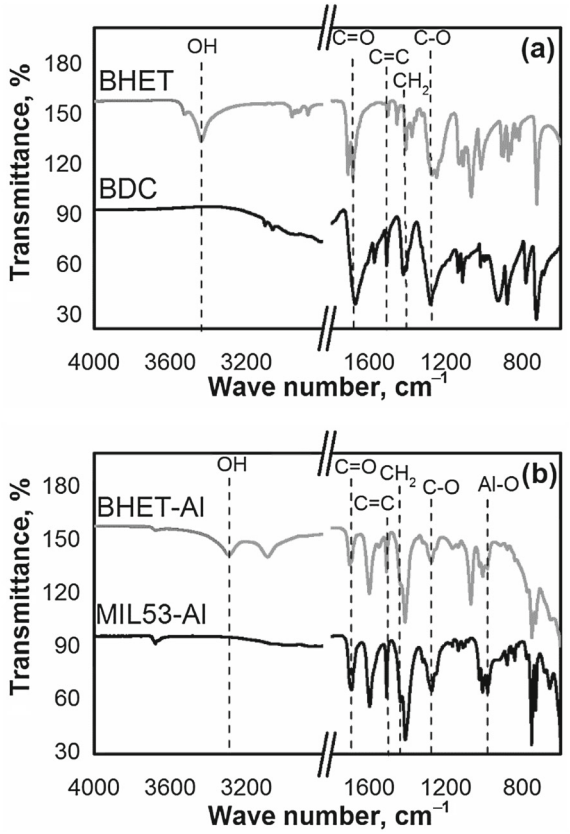

Figure 5. FTIR spectra of (**a**) BDC and BHET organic ligands and (**b**) MIL53-Al and BHET-Al MOFs.

group (C=O) from the carboxylic acid and ester in BDC and BHET, respectively. At ~1280 cm^{-1}, there is a band that is related to the vibration of C–O of the acyl group present in both precursors [7]. The bands at ~3200–3000, ~1680 and ~1500 cm^{-1} are related to the C–H bonds and the C=C stretching vibration, respectively, from the aromatic structure [15]. The intensity of the stretching bands at ~3200–3000 cm^{-1} is higher for the BHET ligand than for the BDC, related to the presence of the ethoxylated skeleton in this PET derivative. Also, at ~1450 cm^{-1}, there is a band in BHET related to methylene groups (–CH_2). Finally, the BHET precursor shows an additional band at ~3430 cm^{-1} associated with hydroxyl groups (-OH) [7].

The ATR–FTIR spectra of MIL53-Al and BHET-Al MOFs (figure 5b) indicated the same functional groups of their organic precursors. But a displacement of the band is also observed in both the materials, related to the carbonyl group from ~1720 to ~1700 cm^{-1} indicating the coordination bond between the aluminium ion and this functional group. Also, there is a band in both materials at ~980 cm^{-1} which is characteristic of the Al–O bond [16]. Furthermore, in BHET-Al MOF, there is a displacement of the band related to hydroxyl groups from ~3430 to ~3280 cm^{-1}, which is attributed to the coordination bond formed by the aluminium ion with the hydroxyl group. The decrement in the intensity of the signals for the vibrations of the C=O and –OH bonds, present in the structure of the BHET-Al, again indicates that these functional groups generate stable coordination interactions with Al^{+3} ions, this is compared with the spectrum of MIL53-Al.

Figure 6 shows the high resolution of XPS spectra of MIL53-Al (left) and BHET-Al (right) of the emissions of C, O and Al elements (from top to bottom). The high-resolution XPS spectrum of C1s and its corresponding deconvolution indicates that the chemical environment of C1s is formed by three centred peaks in both MIL53-Al and BHET-Al. The first peak centred in the binding energy of ~283 eV is related to carbon atoms involved in an Al-O–C complex compound. A second peak at ~284.3 eV is associated with the aromatic carbon of the organic ligands. The third band at ~286 eV is attributed to carbon atoms bonded to carbonyl groups [17].

The high-resolution XPS spectrum of O1s and its corresponding deconvolution exhibits that the chemical environment of O1s is formed by three and four peaks for MIL53-Al and BHET-Al, respectively. The first band centred in the binding energy of ~530.3 eV is associated with the Al–O bond. The second peak centred at ~531.9 eV is attributed to the oxygen of the aromatic carbonyl group. The third peak centred at ~533.6 eV indicates the bond between oxygen and the aromatic carbonyl group. Whereas the additional peak presented in the BHET-Al material at ~532.4 eV indicates the oxygen of the hydroxyl group of the BHET ligand.

The high-resolution XPS spectrum of Al2p and its corresponding deconvolution show that the chemical environment of Al2p is formed by two peaks and three peaks for MIL53-Al and BHET-Al, respectively. The first band centred in the binding energy of ~72 eV is associated with the Al–O bond. The second peak centered at ~75 eV is attributed to the coordination bond between aluminium and the carbonyl group attached to the benzene ring. Whereas the additional peak presented in the BHET-Al material at ~73.7 eV indicates the coordination bond among aluminium and the hydroxyl group of the BHET ligand. The XPS results are in line with that obtained by FTIR, indicating again that the new BHET-Al MOF has stronger coordination bonds since they present higher bonding energy. This is favoured by the synergy produced between the components and its high solubility in the aqueous medium. The energy values of the scattered electrons indicate that the coordination bonds among the aluminium ions and the Lewis bases present in the BHET ligand occur in the coordination sphere that involves the 2p orbitals of the central metal ion, facilitating the diffusion of these ions by ion exchange and favouring adsorption and/or release mechanisms without needing high energy requirements.

For potential biomedical applications of MOFs, it is necessary to evaluate if their chemical structure has cytotoxic effects on cells with biomedical interest. Hence, MIL-53 and BHET-Al were tested by an *in vitro* fibroblasts

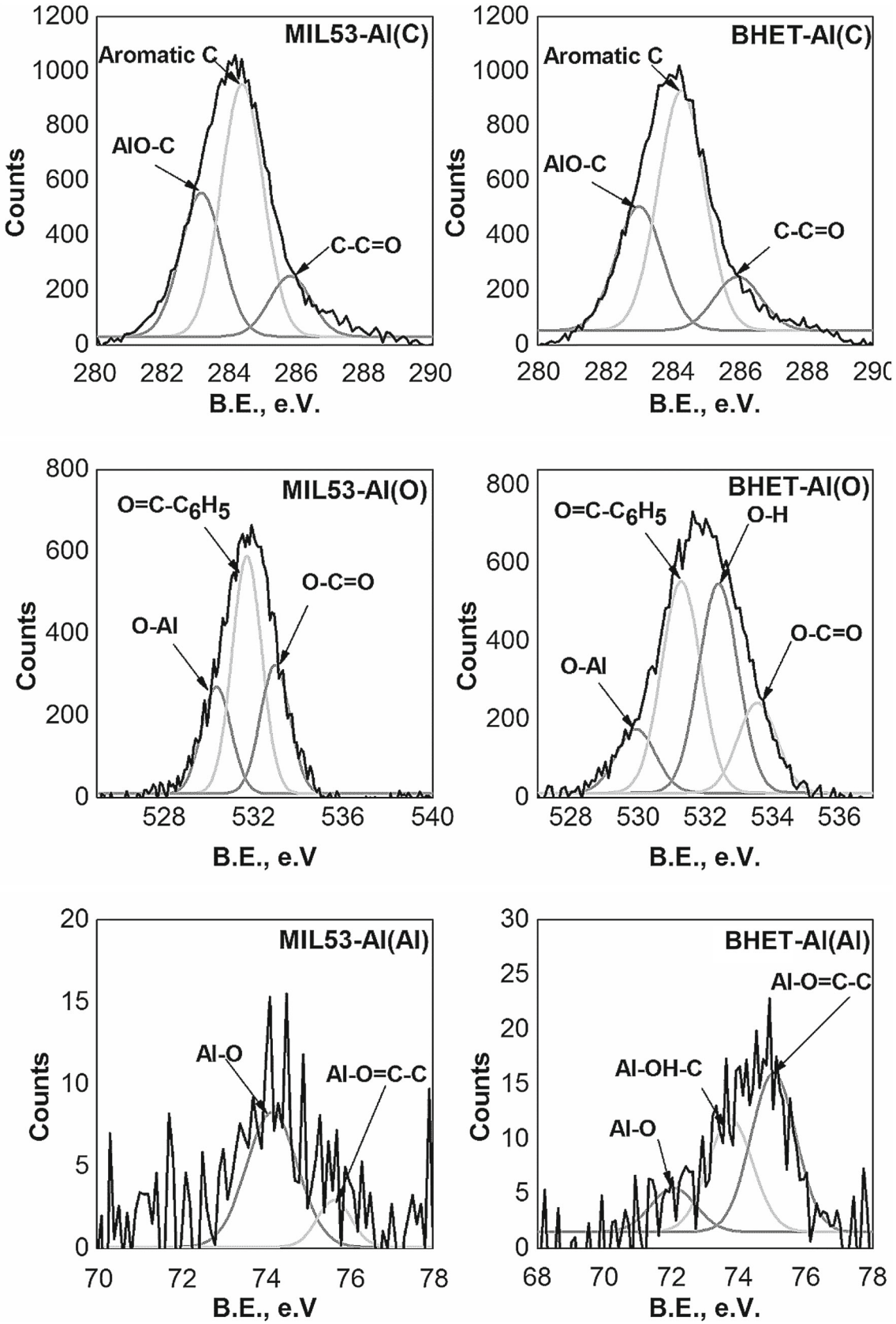

Figure 6. XPS narrow spectra of C1s, O1s and Al2p (from top to bottom) of MIL53-Al (left column) and BHET-Al (right column) MOFs.

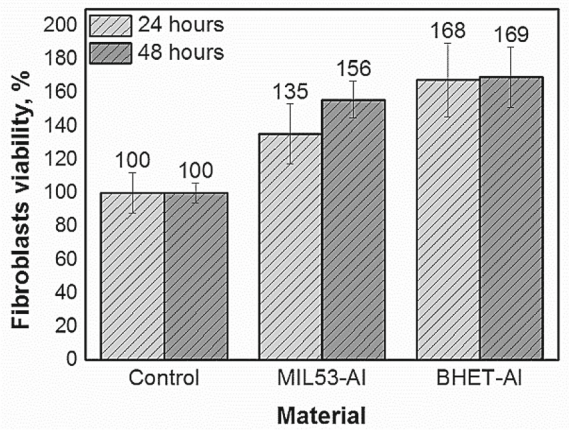

Figure 7. Fibroblasts cell viability in the presence of MOFs.

viability probe, during 24 and 48 h of incubation (figure 7). It is important to notice that the control of fibroblasts metabolism plays a key role in the regeneration of soft tissues, such as skin, cartilage and cornea, benefiting the tissue healing in a minor lapse of time. The results of fibroblasts viability indicate outstanding results for MIL53-Al and BHET-Al MOFs since both materials present viability higher than the control even after 48 h of incubation. Indicating that the chemical structures of the evaluated MOFs do not present cytotoxic effects that decrease the breathing capacity of these cells [18,19].

The cell viability assay directly indicates the mitochondrial function of the cells in the presence of the developed MOFs; if the values are $< 60\%$ viability, it indicates a certain cytotoxic character that affects the respiration activity of the cells, and the values higher than the control (100%) indicate that there are no cytotoxic effects and that the MOFs developed are cytocompatible. This test does not allow evaluating whether there is cellular damage due to high metabolic activity, however, several studies have reported metabolic activities >150% evaluated by the MTT test, thus, determining high cytocompatibility [20–22].

The presence of pores on these structures benefits the regulation of cell functions, ensuring their viability, by the controlled diffusion of oxygen and nutrients, mediated by the porosity of the material. The increase in pore size, determined for BHET-Al shows a significant increment in fibroblast viability, registering a value of 169% at 48 h of incubation. Statistically significant differences are not determined when comparing the fibroblast viability values of the MOFs studied; however, when comparing the viability values of the control with those of BHET-Al, significant differences are determined. In this way, the chemical structure of BHET-Al MOF contributes to significantly increase the respiratory capacity of fibroblasts modifying their metabolism. In biomedical strategies, it is essential that cells actively breathe to ensure tissue healing. On the other hand, the presence of Al^{+3} ions, ensures the inhibition of bacteria that could induce infections at the site of biomedical application, representing materials with optimal properties for successful application in biomedicine.

4. Conclusion

A new MOF from the BHET organic ligand and aluminium ions was synthesized, using a sustainable strategy free of organic solvents. The structure and properties of the new BHET-Al MOF were compared with the representative MIL53-Al MOF. The XRD and SEM analyses indicate that both materials have rhombohedral structures, generating microporous agglomerates of smaller crystals in the case of BHET-Al. The macroporosity of the new MOF is supported by the results of nitrogen physisorption. Besides, the characterization by TGA and FTIR showed higher thermal stability of BHET-Al compared with MIL53-Al, which was attributed to a higher amount of coordination bonds between the aluminium ion and BHET ligand in comparison to BDC ligand. The binding energies analysed by XPS indicate that the coordination bonds presented in this novel material are originated by electrons shared from Lewis bases to the 2p orbitals present in the coordination sphere of the aluminium ion. Interestingly, the chemical structure of the new BHET-Al MOF does not present cytotoxic character for fibroblasts growing on this material for up to 48 h of culture, significantly increasing the cell viability concerning the control, which is an advantage to be applied in biomedical applications. Therefore, the evidence of the present work indicates that BHET is a new organic ligand derived from PET depolymerization; representing a sustainable strategy to generate novel MOFs using water as solvent.

References

[1] Khan N A, Hasan Z and Jhung S H 2018 *Coord. Chem. Rev.* **376** 20
[2] Giménez-Marqués M, Hidalgo T, Serre C and Horcajada P 2016 *Coord. Chem. Rev.* **307** 342
[3] Al-Sabagh A M, Yehia F Z, Eshaq Gh, Rabie A M and El Metwally A E 2016 *Egypt. J. Pet.* **25** 53
[4] Stoski A, Viante M F, Santos Nunes C, Curti Muniz E, Felsner M A and Policiano Almeida C A 2016 *Polym. Int.* **65** 1024
[5] Feng L, Chen R, Hou S, Chen W, Huang H, Wang Y *et al* 2019 *J. Mater. Sci.* **54** 6174
[6] Saska M and Myerson A S 1985 *Cryst. Res. Technol.* **20** 201
[7] Zhou X, Lu X, Wang Q, Zhu M and Li Z 2012 *Pure Appl. Chem.* **84** 789
[8] Sánchez-Sánchez M, Getachew N, Díaz K, Díaz-García M, Chebude Y and Díaz I 2015 *Green Chem.* **17** 1500
[9] Lowell S and Shields J E 1984 *Powder surface area and porosity* (Dordrecht: Springer) p 12

[10] Mounfield W P III and Walton K S 2015 *J. Colloid Interface Sci.* **447** 33
[11] Yang C-X, Ren H-B and Yan X-P 2013 *Anal. Chem.* **85** 7441
[12] Chen X, Hoang V-T, Rodrigue D and Kaliaguine S 2013 *RSC Adv.* **3** 24266
[13] Abid H R, Rada Z H, Shang J and Wang S 2016 *Polyhedron* **120** 103
[14] Sun T, Zhuo Q, Chen Y and Wu Z 2015 *High Perform. Polym.* **27** 100
[15] Wang Y, Kretschmer K, Zhang J, Mondal A, Guo X and Wang G 2016 *RSC Adv.* **6** 57098
[16] Li J, Wu Y-N, Li Z, Zhu M and Li F 2014 *Water Sci. Technol.* **70** 1391
[17] Nguyen T, Tran T, Thi D, Le H, Nguyen O T K, Nguyen V *et al* 2019 *R. Soc. Open Sci.* **6** 190058
[18] Christodoulou I, Serre C and Gref R 2020 In M Mozafari (ed.) *Metal–organic frameworks for biomedical applications* Woodhead Publishing p 467
[19] Pandey A, Dhas N, Deshmukh P, Caro C, Patil P, García-Martín M L *et al* 2020 *Coord. Chem. Rev.* **409** 213212
[20] Cosme-Silva L, Santos A F D, Lopes C S, Dal-Fabbro R, Benetti F, Gomes-Filho J E *et al* 2020 *J. Appl. Oral Sci.* **28** e20200033
[21] Benetti F, Queiroz I O A, Cosme-Silva L, Conti L C, Oliveira S H P and Cintra L T A 2019 *Braz. Dent. J.* **30** 325
[22] Nowakowska D, Kulbacka J, Wezgowiec J, Szewczyk A, Baczynska D, Zietek M *et al* 2021 *Materials* **14** 2081